

**Single impurities in insulators: *Ab initio* study of Fe-doped SrTiO<sub>3</sub>**R. A. Evarestov,<sup>1</sup> S. Piskunov,<sup>2</sup> E. A. Kotomin,<sup>2,3,\*</sup> and G. Borstel<sup>2</sup><sup>1</sup>*Department of Quantum Chemistry, St. Petersburg University, St. Peterhof 198904, Russia*<sup>2</sup>*Fachbereich Physik, Universität Osnabrück, D-49069 Osnabrück, Germany*<sup>3</sup>*Max-Planck-Institut für Festkörperforschung, Heisenbergstrasse 1, Stuttgart D-70569, Germany*  
(Received 11 February 2002; revised manuscript received 3 June 2002; published 6 February 2003)

We present a consistent approach to the study of single (isolated) defects in crystals. This has three stages: (i) band structure calculation of a perfect host crystal is used to define the shape and size of the supercell adequately modeling a perfect crystal, (ii) further supercell point defect calculation for unrelaxed lattice defines a proper cyclic cluster, (iii) the latter is used at the third, the most time-consuming stage for the lattice relaxation and defect property calculations. Using the unrestricted Hartree-Fock (HF) method in the linear combination of atomic orbitals approximation, the calculations of the defect energy level positions in the gap and atomic structure for a single Fe<sup>4+</sup> impurity substituting for a host Ti atom in perovskite SrTiO<sub>3</sub> are performed. We study a convergence of results to the single defect limit and show that use of 160 atom cyclic clusters is necessary for the HF calculations and 320 atoms for the density functional theory PWGGA calculations. The high spin ( $S=2$ ) state is predicted to lie much lower in energy than the zero-spin state. The energy level positions strongly depend on the asymmetric displacement mode of the six nearest O ions which is a combination of the Jahn-Teller and breathing modes. A considerable covalent bonding between the Fe ion and four nearest O ions takes place.

DOI: 10.1103/PhysRevB.67.064101

PACS number(s): 61.72.Ss, 71.15.Ap, 71.20.Be, 74.72.-h

**I. INTRODUCTION**

Properties of transition metal impurities, especially iron, in ABO<sub>3</sub> perovskite ferroelectrics are of considerable interest due to their photochromic, photorefractive and other applications.<sup>1,2</sup> There were several theoretical calculations for ion impurities substituting for B atoms in KNbO<sub>3</sub>,<sup>3,4</sup> SrTiO<sub>3</sub>,<sup>5,6</sup> and BaTiO<sub>3</sub> (Ref. 7) (see more in Ref. 8). Most of these studies were semi-empirical and/or cluster calculations. The only first-principles calculations were performed recently for Fe in KNbO<sub>3</sub> (Ref. 4) using the linear muffin tin orbital method in the atomic sphere approximation (LMTO-ASA). However, no lattice relaxation around the impurity was calculated, and the calculated density of states depends considerably on the parameters of the so-called LDA+U scheme.

In this paper, a consistent and economic approach for defective solids is presented and used for *ab initio* calculations of the iron impurity in SrTiO<sub>3</sub> with a focus on detailed treatment of lattice relaxation around a *single* defect. For perfect crystal we compare results of the periodic Hartree-Fock (HF) and density functional theory (DFT) calculations based on the linear combination of atomic orbitals (LCAO) Gaussian basis sets. For defective crystal the supercell model and Hartree-Fock approximation are used. Despite the fact that supercell approach is widely used already for two decades in defect calculations, very little attention is paid to the supercell size optimization and the effect of periodically repeated defect interaction. A study of the convergence of results to the limit of a single defect is one of main emphases of this paper.

The paper is organized as follows. In Sec. II three stages of the suggested approach realization are considered. Computational details are presented in Sec. III. Results for pure

and Fe-doped SrTiO<sub>3</sub> are analyzed in Secs. IV and V, respectively. Finally, conclusions are summarized in Sec. VI.

**II. A CONSISTENT APPROACH FOR A MODELING OF DEFECTIVE SOLIDS**

Usually defect concentrations in solids are so low that point defects could be treated as single ones. The main problem is to understand changes induced by a single point defect in the electronic and atomic structure of a host crystal (electronic density redistribution, additional local energy levels in the optical gap, lattice relaxation around defects, etc.) This requires use of adequate models for both perfect and defective crystals. When a single point defect appears, perfect crystalline translation symmetry is lost so that use of a **k**-mesh in the Brillouin zone (BZ) and primitive unit cell commonly used in perfect crystal calculations becomes formally impossible. The simplest and direct approach in this case is a *molecular cluster* model of the defective crystal. This is obtained by cutting out in the crystal some fraction of atoms consisting of the point defect and several spheres of nearest neighbors, followed by an embedding this cluster into the field of the surrounding crystal and (or) by saturating cluster dangling bonds with pseudoatoms. There are well-known<sup>9</sup> difficulties of the cluster model connected with changes of host crystal symmetry, pseudoatom choice at the cluster boundaries and the necessity to consider nonstoichiometric (charged) clusters. Nevertheless, a reasonable choice of cluster is possible when well localized point defects are considered.<sup>10</sup>

In recent years, the computer codes for band calculations of crystals became powerful for calculations of solids with quite a large number of atoms in primitive unit cell.<sup>11-14</sup> In this connection, two models alternative to the cluster model became popular. These use the translation symmetry not only

for a perfect but also for defective crystals: the *supercell* model<sup>15,16</sup> (SCM) and the *cyclic cluster* model (CCM). These two models have both similarities and discrepancies.<sup>9,17</sup> Similarity is that in both models not a standard primitive unit cell but an *extended* unit cell is used (this is why it is called *supercell* or also *large unit cell*). Another well-known procedure to treat localized defects exists which is based on the Green's functions method and called the *embedded cluster* model.<sup>18</sup> This model considers a finite cluster including defects embedded into the rest of the host crystal, by assuming that the electronic structure in the external region remains the same as in the perfect crystal. The assumption of locality of the perturbation is exploited differently by different embedding techniques, starting from the pioneering studies of Baraff and Schluter for semiconductors with later extension to ionic systems.<sup>18</sup> The embedding approach is, in principle, more adequate than the SCM, but it is computationally more demanding and also faces convergence problems of the self-consistent procedure (for more details and illustrations see Ref. 19–21). In this paper, we focus on the periodic defect models.

In defect calculations there are two criteria to be met: the model used for solving the quantum mechanical problem has to describe sufficiently well both (i) the extended crystalline states and (ii) the localized states of the isolated defect. The CCM can be defined from the two points of view: it can be regarded either as the application of the Born-Karman cyclic boundary conditions directly to the large unit cell (supercell), or as the band structure calculation on SCM with (a) applying the  $\mathbf{k}=0$  approximation and (b) neglecting interactions beyond the Wigner-Seitz cell corresponding to the supercell. The SCM have no restrictions such as (a) and (b), and thus CCM could be considered as a special approximation to the SCM.

From the viewpoint of criterion (i), approximation (a) is sufficient, provided the primitive  $\mathbf{k}$  vectors represented by the  $\mathbf{k}=0$  point of the narrowed BZ of the supercell form a special  $\mathbf{k}$ -point set of sufficient quality. As for the criterion (ii), the approximation (b) decouples effectively the interactions between periodically repeated atoms of the supercell calculation, provided the change in the charge density, caused by the defect, is negligible at the boundary of the corresponding Wigner-Seitz cell. The problem is, however, that there is no direct way of checking how well these two conditions are satisfied, except, of course, a series of calculations for a trivial, direct increase of the SCM size, which is very time consuming.

In practical self-consistent HF or DFT band structure calculations with the primitive unit cell in direct space the convergence of the bulk electronic properties (total energy per unit cell, band gap, and one-electron energies of band edges, the density of states, and electronic charge distribution) can be obtained by increasing the number of the used  $\mathbf{k}$  points in the primitive BZ. The speed of this convergence and a final number of necessary  $\mathbf{k}$  points depend on the particular system under consideration, basis set used, etc. When performing the BZ summation, theory of so-called *special*  $\mathbf{k}$  points in the BZ is widely used.<sup>22</sup> The one-to-one correspondence was demonstrated<sup>23–25</sup> between any fixed  $\mathbf{k}$  mesh and the super-

cell in a real space, defined by its translation vectors

$$\mathbf{A}_j = \sum_{i=1}^3 l_{ij} \mathbf{a}_i \quad (1)$$

with the translation vectors of the primitive cell  $\mathbf{a}_i$ , and its volume  $V_a = \mathbf{a}_1[\mathbf{a}_2 \times \mathbf{a}_3]$ ,  $\det l = L$ ,  $i, j = 1, 2, 3$ .

Here  $L > 1$  means a number of primitive unit cells in the corresponding supercell. Introducing a supercell, defined by Eq. (1), one receives from the equation below the corresponding mesh  $\{\mathbf{k}_i\}$  of the  $\mathbf{k}$  points in the BZ

$$\exp(-i\mathbf{k}_i \cdot \mathbf{A}_j) = 1, \quad j = 1, 2, 3 \quad t = 1, 2, \dots, L. \quad (2)$$

The absolute value  $R_M$  of the smallest  $\mathbf{A}_j$  in Eq. (1) defines the accuracy of the special points set chosen and might be called *cutoff length* for any  $\mathbf{k}$  mesh. Each  $R_M$  may be characterized by some number of spheres  $M$  of the lattice translation vectors ordered in such a way that the sphere radii are not decreasing.<sup>24,26</sup>

It is possible to choose the matrix  $l$  in Eq. (1) both diagonal and nondiagonal but maintaining the point symmetry of the crystalline lattice.<sup>23</sup> By increasing  $L$ , one can ensure increase of  $\mathbf{k}$ -mesh accuracy and thus the accuracy of the corresponding supercell modeling the perfect crystal.

Using Wannier functions in one-electron density matrix (DM) definition, it was shown<sup>17,27,28</sup> that the convergence of the self-consistent results with an increase of the  $\mathbf{k}$ -mesh accuracy takes place when the diagonal DM elements (used in DFT calculations) decay to zero at the cutoff length  $R_M$ . In the HF method (due to its nonlocal exchange) the calculated off-diagonal DM elements (between the reference primitive cell and that centered at the lattice site on the sphere of the radius  $R_M$ ) must decay to zero.

Thus, one can say that an increase of  $\mathbf{k}$ -mesh accuracy in self-consistent band structure calculations with primitive cell means in fact that the perfect crystal is modeled by a *sequence* of supercells of the increasing size. The convergence of the results (size of the converged supercell) depends on the system under consideration (for small or zero-band gap crystals convergence is very slow, but for ionic crystals already relatively moderate  $\mathbf{k}$  meshes are sufficient, as we show below for the case of a wide-gap SrTiO<sub>3</sub> crystal).

Use of SCM means, in fact, consideration of a “new crystal” with artificially introduced point defect periodicity. The point defect period is defined by the supercell choice, the space group of a defective crystal in SCM is defined by the local point symmetry of a defect and the chosen lattice of supercells.<sup>17,29,30</sup> The calculation is made in the same way as for a perfect crystal using the  $\mathbf{k}$  sampling of the BZ [note that a new, narrowed BZ is  $L$ -times smaller than the original (primitive) one and may differ when the type of lattice is changed by the transformation, Eq. (1)]. In practical calculations those  $\mathbf{k}$  sets are used which allow to minimize the defect-defect interaction<sup>13</sup> for a fixed supercell size and shape.

Use of the  $\mathbf{k}$  meshes in SCM allows one to estimate for each supercell chosen the role of defect-defect interaction

through the width of the defect energy bands: the narrower these bands are, the closer the results obtained are to the single defect limit. When the convergence is reached, SCM gives the same results as CCM for the same  $l$ -matrix choice in Eq. (1). Unfortunately, SCM faces the following difficulties: the lattice relaxation around the defect is periodically repeated which affects the total energy per cell, for charged point defects artificial periodicity requires use of some charge compensation. These difficulties are absent in CCM.

We suggest in this paper the economic approach to a single point defect study, consisting of three stages. At stage 1 the band structure calculation of a perfect crystal is performed, in order to fix the shape and size of the supercell which reasonably models the host crystal, i.e., when the above-described condition (i) is met. These calculations are made using primitive unit cell and  $\mathbf{k}$  sampling in the usual (primitive) BZ. Due to abovementioned one-to-one correspondence between  $\mathbf{k}$ -point sampling and the supercell size in a real space, it is possible to find such a  $\mathbf{k}$  mesh which ensures a compromise between its size and a reasonable reproduction of the total and one-electron energies, as well as the electron density distribution in the host crystal. At this stage the  $\mathbf{k}$ -point sets satisfying Eq. (2) are used.

At stage 2 the calculations are made for a *defective* crystal using SCM, in order to check the above-described criterion (ii). It is reasonable to begin from the smallest supercell, chosen at stage 1, i.e., corresponding to the converged results of the band calculations. In the particular case of the SrTiO<sub>3</sub> crystal supercell of 80 atoms may be used for a perfect crystal in the HF calculations (see Sec. IV) but larger supercells are necessary in the DFT-PWGGA calculations. When estimating at the second stage the defect-defect interaction from the calculated defect band width, one makes a decision about the need of a further increase of the supercell. As it will be shown below, the iron band width in the HF calculations still changes when supercell is increased from 80 to 160 atoms. It means that the local states induced by the point defect are sufficiently well localized only in the larger, 160-atom supercell. That is, at stage 2 the comparison of supercell results for different  $\mathbf{k}$  meshes allows one to decide if it is necessary to further increase a supercell, in order to surpass artificial defect-defect interaction. When energies at  $\mathbf{k}=0$  and non-zero  $\mathbf{k}$  supercell calculations turn out to be close, this means that the corresponding *cyclic cluster* is chosen for the isolated defect study.

At the most time-consuming stage 3 the CCM is used (i.e., performing band structure calculations for the chosen supercell only at  $\mathbf{k}=0$ ) for the relaxation of the crystalline lattice around the point defect and calculation of other defective crystal properties. In particular, different charge states of the point defect could be also considered without difficulties since in CCM the charge is not periodically repeated over the lattice. The results of CCM calculations of SrTiO<sub>3</sub>-Fe with lattice relaxation are discussed in Sec. V. To our opinion, this approach guarantees a correct study of the convergence to the limit of a single defect.

Let us illustrate what was said above for the simple cubic (sc) lattice of perovskite-type ABO<sub>3</sub> structure. The 2<sup>3</sup>

$\mathbf{k}$ -point Monkhorst-Pack mesh<sup>31</sup> consists of eight points in the BZ and corresponds to the transformation (1) with the following diagonal matrix:

$$l = \begin{pmatrix} 2 & 0 & 0 \\ 0 & 2 & 0 \\ 0 & 0 & 2 \end{pmatrix}.$$

In the irreducible part of the BZ this  $\mathbf{k}$  mesh consists of four points  $\Gamma$  (000),  $R(\frac{1}{2} \frac{1}{2} \frac{1}{2})$ ,  $M(\frac{1}{2} \frac{1}{2} 0)$ ,  $X(\frac{1}{2} 0 0)$  (in units of the reciprocal lattice basic translations,  $M$  and  $X$  points form three-branch stars in the whole BZ). The corresponding supercell in the real space consists of eight primitive unit cells, for SrTiO<sub>3</sub> perovskite this results in  $5 \times 8 = 40$  atoms. Next  $\mathbf{k}$  meshes based on the diagonal transformation matrix, (1) correspond to  $4 \times 4 \times 4 = 64$  and  $6 \times 6 \times 6 = 216$   $\mathbf{k}$  points in the BZ, with the relevant supercells of 320 and 1080 atoms, respectively.

However, the transformation, (1) could also be done for nondiagonal  $l$  matrices

$$\begin{pmatrix} 1 & 1 & 0 \\ 1 & 0 & 1 \\ 0 & 1 & 1 \end{pmatrix}, L=2 \quad \text{and} \quad \begin{pmatrix} 1 & 1 & -1 \\ 1 & -1 & 1 \\ -1 & 1 & 1 \end{pmatrix}, L=4$$

which result in the fcc and bcc lattices, respectively.

The corresponding  $\mathbf{k}$  sets are the  $\Gamma$ ,  $R$  and  $\Gamma$ ,  $3M$ , respectively. Further  $2 \times 2 \times 2$  increase of the unit cells for these two lattices gives the  $\mathbf{k}$  meshes corresponding to the supercells of  $L=16$  and  $L=32$  primitive unit cells (80 and 160 atoms, respectively.) At last, the  $\mathbf{k}$  mesh with  $L=108$  ( $3 \times 3 \times 3$  extension of the bcc lattice with  $L=4$ ) corresponds to the supercells of 540 atoms.

Thus, at the first stage the band calculation of a perfect SrTiO<sub>3</sub> crystal is made for the  $\mathbf{k}$  meshes received for transformations (1) and (2), with  $L=8, 16, 32, 64, 108$  (these meshes are easily generated by our small computer code) and the convergence of the results for host crystal is investigated. The relevant sets of the  $\mathbf{k}$  meshes in the BZ are as follows:

$$\mathbf{L8}(\Gamma, R, 3M, 3X), \quad \text{where } \Gamma(0,0,0)R\left(\frac{1}{2}, \frac{1}{2}, \frac{1}{2}\right),$$

$$M\left(\frac{1}{2}, \frac{1}{2}, 0\right), X\left(\frac{1}{2}, 0, 0\right), \quad (3)$$

$$\mathbf{L16}(\Gamma, R, 3M, 3X, 8\Lambda), \quad \text{i.e., as } L8 \quad \text{and } \Lambda\left(\frac{1}{4}, \frac{1}{4}, \frac{1}{4}\right),$$

$$\mathbf{L32}(\Gamma, R, 3M, 3X, 12\Sigma, 12S), \quad \text{i.e., as } L8 \quad \text{and}$$

$$\Sigma\left(\frac{1}{4}, \frac{1}{4}, 0\right), S\left(\frac{1}{4}, \frac{1}{4}, \frac{1}{2}\right),$$

TABLE I. Convergence of results for pure SrTiO<sub>3</sub> ( $a_0=3.905 \text{ \AA}$ ) obtained for pure HF (a) and DFT-PWGGA (b) band calculations corresponding to cyclic clusters of an increasing size. All energies in eV, total energies are presented with respect to the reference point of 80 a.u.=2176.80 eV.  $q$  and  $V$  are effective atomic charges and valencies (in  $e$ ), respectively.  $L, N_A$ , are the primitive unit cell extension, a number of atoms in the cyclic cluster, whereas  $R_M$  and  $M$  are defined by Eqs. (1) and (4), respectively.

$L, N_A$	Matrix	$M$	$R_M(\text{\AA})$	$E_{\text{tot}}, \text{eV}$	(a) HF calculations							
					$\varepsilon_v, \text{eV}$	$\varepsilon_c, \text{eV}$	$q(\text{Ti})$	$q(\text{O})$	$q(\text{Sr})$	$V(\text{Ti})$	$V(\text{O})$	$V(\text{Sr})$
8, 40 (sc)	A	4	7.81	-24.288	-6.838	3.393	2.39	-1.41	1.84	3.94	2.07	2.01
16, 80 (fcc)	B	7	11.04	-24.818	-6.895	3.766	2.54	-1.46	1.84	3.97	2.06	2.01
32, 160 (bcc)	C	11	13.53	-24.873	-6.906	3.725	2.54	-1.46	1.84	3.98	2.06	2.01
64, 320 (sc)	D	14	15.62	-24.873	-6.906	3.720	2.54	-1.46	1.84	3.98	2.06	2.01
108, 540 (bcc)	E	24	20.29	-24.883	-6.895	3.744	2.54	-1.46	1.84	3.98	2.06	2.01

$L, N_A$	Matrix	$M$	$R_M(\text{\AA})$	$E_{\text{tot}}, \text{eV}$	(b) DFT-PWGGA calculations							
					$\varepsilon_v, \text{eV}$	$\varepsilon_c, \text{eV}$	$q(\text{Ti})$	$q(\text{O})$	$q(\text{Sr})$	$V(\text{Ti})$	$V(\text{O})$	$V(\text{Sr})$
8, 40 (sc)	A	4	7.81	-73.059	-4.647	4.367	3.43	-1.74	1.79	3.98	2.06	2.04
16, 80 (fcc)	B	7	11.04	-73.024	-2.735	2.169	2.82	-1.51	1.71	3.97	2.09	2.04
32, 160 (bcc)	C	11	13.53	-70.874	-2.737	1.219	2.55	-1.42	1.70	3.99	2.11	2.04
64, 320 (sc)	D	14	15.62	-66.101	-2.414	0.027	1.69	-1.13	1.70	4.12	2.18	2.04
108, 540 (bcc)	E	24	20.29	-66.134	-2.443	-1.025	1.69	-1.13	1.70	4.12	2.18	2.04

Transformation matrices, Eq. (1)

$$A = \begin{pmatrix} 200 \\ 020 \\ 002 \end{pmatrix}, B = \begin{pmatrix} 220 \\ 202 \\ 022 \end{pmatrix}, C = \begin{pmatrix} 22-2 \\ 2-22 \\ -222 \end{pmatrix}, D = \begin{pmatrix} 400 \\ 040 \\ 004 \end{pmatrix}, E = \begin{pmatrix} 33-3 \\ 3-33 \\ -333 \end{pmatrix}$$

**L64**( $\Gamma, R, 3M, 3X, 12\Sigma, 12S, 8\Lambda, 6\Delta, 6T, 12Z$ ), i.e., as **L32**

$$\text{and } \Delta \left( \frac{1}{4}, 0, 0 \right), T \left( \frac{1}{4}, \frac{1}{2}, \frac{1}{2} \right), Z \left( \frac{1}{4}, \frac{1}{2}, 0 \right),$$

$$\Lambda \left( \frac{1}{4}, \frac{1}{4}, \frac{1}{4} \right),$$

**L108**( $\Gamma, 3M, 6\Delta, 6T, 12\Sigma, 12\Sigma', 8\Lambda, 12Z, 24B, 24C$ ),

$$\text{where } \Delta \left( \frac{1}{3}, 0, 0 \right), T \left( \frac{1}{3}, \frac{1}{2}, \frac{1}{2} \right), \Sigma \left( \frac{1}{3}, \frac{1}{3}, 0 \right),$$

$$\Sigma' \left( \frac{1}{6}, \frac{1}{6}, 0 \right), \Lambda \left( \frac{1}{3}, \frac{1}{3}, \frac{1}{3} \right); Z \left( \frac{1}{6}, \frac{1}{2}, 0 \right),$$

$$B \left( \frac{1}{6}, \frac{1}{2}, \frac{1}{3} \right), \text{ and } C \left( \frac{1}{6}, \frac{1}{6}, \frac{1}{3} \right).$$

The transformation matrices defined by Eq. (1) for these  $\mathbf{k}$ -point sets are given in Table I. These special  $\mathbf{K}_q$  points sets satisfy the well known Chadi-Cohen condition<sup>22</sup>

$$\sum_{\mathbf{K}_q} w_q \sum_{|\mathbf{R}_j|=d_m} \exp(i\mathbf{K}_q \cdot \mathbf{R}_j) = 0, m=0,1,2,3,\dots, \quad (4)$$

where the second lattice sum is over lattice vectors of the same length equal with the  $m$ th neighbor distance  $d_m$ , the first sum is over a set of these special  $\mathbf{K}_q$  points, and  $w_q$  are weighting factors equal to the number of branches in their

stars. The larger the number  $m$ , the better is the electronic density approximation for the perfect crystal. The numbers  $M$  ( $m=0,1,2,\dots,M-1$ ), defining according to Eq. (4) the accuracy of the corresponding  $\mathbf{K}_q$  sets, Eq. (3), are given in Table I.

### III. COMPUTATIONAL DETAILS

The *ab initio* periodic restricted and unrestricted Hartree-Fock (RHF, UHF) calculations were performed for perfect and defective SrTiO<sub>3</sub> crystals, respectively, using the CRYSTAL computer code.<sup>11</sup> This code has the unique option to perform both HF and DFT calculations on equal grounds, for a large number of implicitly or *a posteriori* used exchange-correlation functionals which permits one to analyze directly the relevant electron correlation effects keeping other computational conditions the same. The crystalline orbitals used in HF calculations as the basis set for the wave function expansion are constructed from a linear combination of atom-centered Gaussian orbitals (HF-LCGO approximation). The same basis set was used in our DFT calculations with Perdew-Wang exchange-correlation functional,<sup>32</sup> taking into account generalized gradient correlation corrections (DFT-PWGGA) to the electron density.

For perfect crystal we compare results for pure HF, HF with *a posteriori* DFT corrections, using PW-GGA functional (hereafter, HF-PWGGA) and lastly, Kohn-Sham equations as implemented into the DFT-PWGGA scheme. A critical review of *a posteriori* DFT corrections to the HF total

energy calculations was presented in Ref. 33. Note that the CRYSTAL-98 code was earlier successfully used for a study of many oxides, including perovskite crystals.<sup>34,35</sup>

We used large core (LC) Durand-Barthelat<sup>36</sup> pseudopotentials for Ti and O atoms and Hay-Wadt small-core pseudopotentials for Sr atoms.<sup>37</sup> The impurity iron atoms were treated as all electron atoms. The “standard” basis for Ti and O was taken from previous TiO<sub>2</sub> CRYSTAL calculations,<sup>38</sup> whereas that for Fe and Sr from Refs. 11, 39. We also made calculations for a reoptimized basis set. For this purpose we used the code developed by Heifets and based on a total energy minimization in CRYSTAL code by means of the conjugated gradient method. As a result, the Ti *5sp* and O *4sp* basis functions are more delocalized (the orbital exponents are changing from 0.4840 Bohr<sup>-2</sup> to 0.4608 and 0.2811 to 0.2667, respectively) which, however, gives only a small energy gain per cell of 0.007 eV. Fe basis set optimization resulted in a larger energy gain of 0.07 eV.

The calculation *thresholds*  $N$  (i.e., the calculation of integrals with an accuracy of  $10^{-N}$ ) were chosen as a compromise between the accuracy of the calculations and the large computational time for large cells (see below). They are 6, 6, 6, 6, and 12 for the Coulomb overlap, Coulomb penetration, exchange overlap, the first exchange pseudo-overlap, and for the second exchange pseudo-overlap, respectively.<sup>11</sup>

To characterize the chemical bonding and covalency effects for both defective and perfect crystals, we used a standard Mulliken population analysis for the effective atomic charges  $q$  and other local properties of electronic structure (bond orders, atomic covalencies, and full valencies).<sup>38,40</sup> The *bond orders* between atoms  $A$  in 0 unit cell and  $B$  in the  $n$ th cell

$$W_{A0,Bn} = \sum_{\mu \in A} \sum_{\lambda \in B} [(PS)_{\mu\lambda}^{A0,Bn} (PS)_{\lambda\mu}^{Bn,A0} + (P^S S)_{\mu\lambda}^{A0,Bn} (P^S S)_{\lambda\mu}^{Bn,A0}], \quad (5)$$

where  $P = P^\alpha + P^\beta$  is the total electron density matrix,  $P^S = P^\alpha - P^\beta$  is the spin density matrix,  $S$  overlap matrix,  $\mu, \nu$  are orbitals on atoms  $A$  and  $B$ . In RHF calculations  $P^\alpha = P^\beta$ .

In calculations with nonzero  $\mathbf{k}$  vectors  $\alpha$  and  $\beta$  matrix elements are defined as

$$(P_{\mu\nu}^{\alpha(\beta)} S)_{\lambda\mu}^{A0,Bn} = \frac{1}{L} \sum_{\mathbf{k}} [P^{\alpha(\beta)}(\mathbf{k}) S(\mathbf{k})]_{\lambda\mu} \exp(-i\mathbf{k} \cdot \mathbf{R}_n), \quad (6)$$

$$P_{\mu\nu}^{\alpha(\beta)}(\mathbf{k}) = \sum_i^{\text{occ}} C^{\alpha(\beta)}_{i\mu}(\mathbf{k}) C_{i\nu}^{\alpha(\beta)}(\mathbf{k}), \quad (7)$$

and

$$S_{\mu\nu}(\mathbf{k}) = \sum_n \exp(-i\mathbf{k} \cdot \mathbf{R}_n) \int \varphi_\mu^*(\mathbf{r} - \mathbf{R}_A) \times \varphi_\nu(\mathbf{r} - \mathbf{R}_B - \mathbf{R}_n) d\mathbf{r}, \quad (8)$$

where  $\mathbf{R}_A, \mathbf{R}_B$  are vectors defining atom  $A$  and  $B$  positions in primitive unit cell.

The *atom covalency*  $C_A$  in a crystal was defined by us as a sum of all bond orders of this atom

$$C_{A0} = \sum_{B \neq A} W_{A0,B0} + \sum_{n \neq 0} \sum_B W_{A0,Bn}. \quad (9)$$

Using the idempotency of the spin-density matrices  $P^\alpha$  and  $P^\beta$ , the following expression could be easily obtained:

$$(PS)^2 = 2(PS) - (P^S S)^2 \quad (10)$$

so that covalency  $C_A$  may be expressed through an electron population  $N_A$  of an atom  $A$  and one center matrix elements of density matrix

$$C_A = 2N_A - P_{A0,A0}, N_A = \sum_{\mu \in A} (PS)_{\mu\mu}^{A0,A0}. \quad (11)$$

The effective charge on the atom is

$$q_A = Z_A - N_A, \quad (12)$$

where  $Z_A$  is the nuclear charge.

Lastly, the *total valence* of an atom,<sup>38</sup> taking into account both ionic and covalent components of the chemical bonding could be expressed through the covalency  $C_A$  and the effective atomic charge  $q_A$

$$V_A = \frac{1}{2} (C_A + \sqrt{C_A^2 + 4q_A^2}). \quad (13)$$

It was shown, indeed, for titanium crystalline oxides<sup>38</sup> that the oxidation state of a metal atom correlates well with the calculated total valence of atom  $V_A$ .

#### IV. RESULTS FOR PERFECT SrTiO<sub>3</sub> AND SUPERCELL CONVERGENCE

Since the lattice relaxation calculations around a point defect is one of our aims, we start with analysis of the ability of three calculation schemes (HF, HF-PWGGA, and DFT-PWGGA) to reproduce the experimental lattice constant  $a_0$  and bulk modulus  $B$  for a perfect SrTiO<sub>3</sub> crystal. With “standard” basis for  $\mathbf{K}_q$  set Eq. (4), we performed band structure calculations with  $6 \times 6 \times 6$  points in BZ ( $M = 34$ ). We obtained  $a_0 = 3.92, 3.84,$  and  $3.92 \text{ \AA}$ , for HF, HF-PWGGA, and DFT-PWGGA, respectively. The experimental value is  $a_0 = 3.905 \text{ \AA}$ . The bulk moduli are  $B = 222, 242,$  and  $195 \text{ GPa}$ , respectively, to be compared with the experimental value (extrapolated to 0 K)  $B = 180 \text{ GPa}$ .<sup>41</sup> That is, pure HF gives an error of 0.5% only for the lattice constant, and by 20% overestimates the bulk modulus. Its *a posteriori* electron correlation correction, HF-PWGGA, gives  $a_0$  too small, and  $B$  even larger than the pure HF. Use of our optimized basis set results in  $a_0 = 3.93, 3.85,$  and  $3.93 \text{ \AA}$  for HF, HF-PWGGA, and DFT-PWGGA, respectively. The relevant bulk moduli are  $B = 220, 249,$  and  $191 \text{ GPa}$ , respectively. That is, the basis optimization only slightly affected calculated  $a_0$  and  $B$  values.

Tables Ia and Ib demonstrate the effect of the cyclic

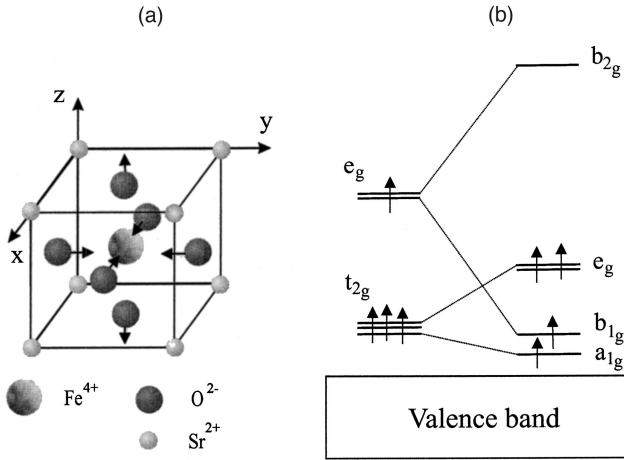


FIG. 1. (a) Schematic view of the Fe impurity with asymmetric  $e_g$  relaxation of six nearest O atoms. (b) The relevant energy levels before and after relaxation.

cluster increase for both pure HF and DFT-PWGGA methods, respectively. The main calculated properties are: the total energy (per primitive unit cell), one-electron band edge energies of the valence band top and conduction band bottom  $\varepsilon_v$  and  $\varepsilon_c$ , Mulliken effective atomic charges  $q$  and atomic valencies, Eq. (13). As is well seen, the result convergence, as the supercell size increases, is quite different for the HF and DFT. We explain much slower DFT convergence by more covalent calculated electron charge distribution, as compared to the HF case. For both methods the convergence of local properties of the electronic structure (atomic charges and valencies) is faster than that for the total and one-electron energies.

Based on results of Table I, the conclusion can be drawn that in the HF calculations of perfect crystal, the electronic structure is reasonably well reproduced by the supercell of 80 atoms ( $L=16$ ). This is confirmed by the band structure

TABLE II. The width of the Fe impurity band  $E_W$  (in eV) calculated for the relevant supercells.

Supercell	No. atoms	Fe-Fe distance ( $\text{\AA}$ )	$E_W$ , eV
L8	40	7.81	1.42
L16	80	11.04	0.23
L32	160	13.53	0.14

analysis. The results of the standard band structure calculations for the SrTiO<sub>3</sub> primitive unit cell with Pack-Monkhorst  $\mathbf{k}$  set  $6 \times 6 \times 6$  and the cyclic cluster of 80 atoms ( $\mathbf{k}=0$ ) are very similar. (In the latter case the symmetry points of the BZ correspond to direct fcc lattice.) It appears that the most important features of the electronic structure of a perfect crystal (valence and conduction band widths, local properties of electronic structure) are well reproduced at the  $\Gamma$  point of the cyclic cluster. The corresponding one-electron energies do not practically change along all symmetry directions in the narrowed BZ.

Analysis of the difference electron density plots, calculated for the primitive unit cell with the  $\mathbf{k}$  set  $6 \times 6 \times 6$ , and for the 80 atom cyclic cluster confirms that the latter well reproduces the electron density distribution in a perfect crystal. Lastly, the total and projected density of states for a perfect crystal show that the upper valence band consists of O  $2p$  atomic orbitals with admixture of Ti  $4d$  orbitals, whereas the Sr states contribute mainly to the energies close to the conduction band bottom, in agreement with previous studies.<sup>3</sup> However, as follows from Table I, very accurate modeling of pure SrTiO<sub>3</sub> by means of DFT-PWGGA needs use of the cyclic clusters as big as 320 atoms ( $L=64$ ). Unfortunately, this is beyond of our current computer facilities. Therefore, we performed below only the HF calculations for Fe impurity using 80 and 160 atom cyclic clusters ( $L=16$  and 32).

TABLE III. Effective charges  $q$  of ions obtained in the HF band structure calculations with Pack-Monkhorst  $k$  set  $6 \times 6 \times 6$  and different cyclic clusters modeling perfect and defective SrTiO<sub>3</sub>. The lengths in the first column are lattice constants of the relevant supercells whereas the distances  $R$  given above the effective charges are calculated with respect to the supercell coordinate origin where the Fe ion is placed.

$R$ , $\text{\AA}$	0.00	1.95	3.38	3.90	4.37	5.52	5.86	6.48	6.76	7.04	7.81
Lattice const. $\text{\AA}$	$q(\text{Fe})$	$q(\text{O})$	$q(\text{Sr})$	$q(\text{Ti})$	$q(\text{O})$	$q(\text{Ti})$	$q(\text{O})$	$q(\text{Sr})$	$q(\text{Ti})$	$q(\text{O})$	$q(\text{Ti})$
3.90		-1.458	1.837	2.538							
band structure, perfect crystal											
15.62		-1.459	1.837	2.540	-1.459	2.540	-1.459	1.837	2.540	-1.459	2.540
L64, perfect crystal											
7.81	2.583	-1.464	1.835	2.406							
L8											
11.04	2.571	-1.464	1.840	2.536	-1.460	2.543					
L16											
13.53	2.570	-1.464	1.838	2.534	-1.458	2.540	-1.459	1.837	2.540		
L32											
15.62	2.570	-1.463	1.838	2.534	-1.458	2.540	-1.459	1.837	2.540	-1.459	2.539
L64											

TABLE IV. Positions of one-electron Fe levels (in eV) with respect to the VB top calculated by means of HF method for  $L = 16$  and  $L = 32$  cyclic cluster with and without lattice relaxation.

Cyclic Cluster	Before relaxation		After relaxation			
	$t_{2g}$	$e_g$	$a_{1g}$	$b_{1g}$	$e_g$	$b_{2g}$
80 atoms	0.36	2.31	0.02	0.03	0.5	5.4
160 atoms	0.25	2.50	0.02	0.05	0.5	5.0

## V. RESULTS FOR A SINGLE Fe IMPURITY

Figure 1(a) shows schematically the iron atom substituting for a host Ti atom and surrounded by six nearest neighbor (NN) O ions in face-centered positions. Table I has shown that an increase of the cyclic cluster from  $L16$  to  $L32$  does not change the HF-calculated top of the valence band. However, the calculated width of the *defect* impurity band  $E_w$  found using our standard Monkhorst-Pack set  $6 \times 6 \times 6$  for three different supercells (Table II), demonstrates clearly a considerable dispersion of defect energies across the BZ. Indeed, the  $E_w$  decreases rapidly, from 1.42 eV ( $L8$ ) down to 0.23 eV ( $L16$ ), and further down to 0.14 eV ( $L32$ ), when the Fe-Fe distance increases only by a factor of about 2, from 7.81 to 13.53 Å, since an overlap of the impurity atomic functions decreases exponentially. This is why only  $L32$  (160 atom) cyclic cluster is suitable for a careful modeling of the *single* Fe impurity and lattice relaxation around it. This is in contrast with many previous supercell calculations of defects where  $L8$  supercells were often used without any convergence analysis.

Mulliken effective charges calculated for ions at different positions in supercells modeling pure and Fe-doped  $\text{SrTiO}_3$  are summarized in Table III. Its first two lines demonstrate that the standard band structure calculation and the  $L64$  cyclic cluster give essentially identical charges. The more so, charges of the same ions in 320 atom supercell are the same, irrespective of the ion position inside the cyclic cluster. Next, in the defective crystal calculations, say, for the  $L32$  cyclic cluster, the effective charges of atoms close to its boundary are the same as in the perfect crystal. This confirms that the chosen cyclic cluster is large enough.

The  $L32$ -UHF supercell calculations for the zero-spin and high-spin ( $S=2$ ) states show that the latter is much lower in energy (by 5.4 eV) (after lattice relaxation). In the perovskite crystalline field a five-fold degenerate Fe  $3d$  state splits into  $e_g$  and  $t_{2g}$  states [Fig. 1(b)] separated by 2.1 eV (for an undistorted lattice). In the high spin state with  $S=2$  the upper  $e_g$  level is occupied by one  $\alpha$  electron and three other  $\alpha$  electrons occupy  $t_{2g}$  states. As is well known<sup>3,4</sup> in this case an  $E_g \otimes e_g$  Jahn Teller effect takes place. This means that an orbital degeneracy is lifted by an *asymmetrical*  $e_g$  displacement of six O ions, as shown in Fig. 1(a): four equatorial O atoms lying in the  $x$ - $y$  plane relax towards the impurity, whereas the two other O ions relax outwards along the  $z$  axis. This results in two nondegenerate levels close to the valence band top:  $e_g$  level at 0.5 eV above the band, and a virtual nondegenerate  $b_{2g}$  level lying much higher (Table IV).

If we assume that  $x$ ,  $y$ ,  $z$  displacements have equal mag-

TABLE V. The effective Mulliken charges of atoms  $q$  and bond orders  $W$  (in  $e$ ) for the  $L32$  HF cyclic cluster with unrelaxed and relaxed lattices.

$\text{SrTiO}_3$	$q$ (Ti)	$q(\text{O}_{x,y})$	$q(\text{O}_z)$	$W$ (Ti-O <sub>x</sub> )	$W$ (Ti-O <sub>z</sub> )
Pure	2.540	-1.459	-1.459	0.375	0.375
Fe-doped	$q(\text{Fe})$	$q(\text{O}_{x,y})$	$q(\text{O}_z)$	$W$ (Fe-O <sub>x</sub> )	$W$ (Fe-O <sub>z</sub> )
Unrelaxed	2.570	-1.464	-1.464	0.164	0.164
Relaxed	2.594	-1.440	-1.534	0.235	0.154

nitudes, pure HF and HF-PWGGA calculations with the “standard” basis set give practically the same magnitude of the six O displacements  $\delta=0.04$  Å, a quite flat minimum and an energy gain of 1.40 eV. This means that we have a *combination* of the Jahn-Teller and breathing modes of surrounding O atom displacements. With our optimised basis set we obtained the energy gain slightly smaller, 1.33 eV. We have checked also whether the magnitudes of the O atom displacements along the  $x$ ,  $y$  and the  $z$  axes could be different

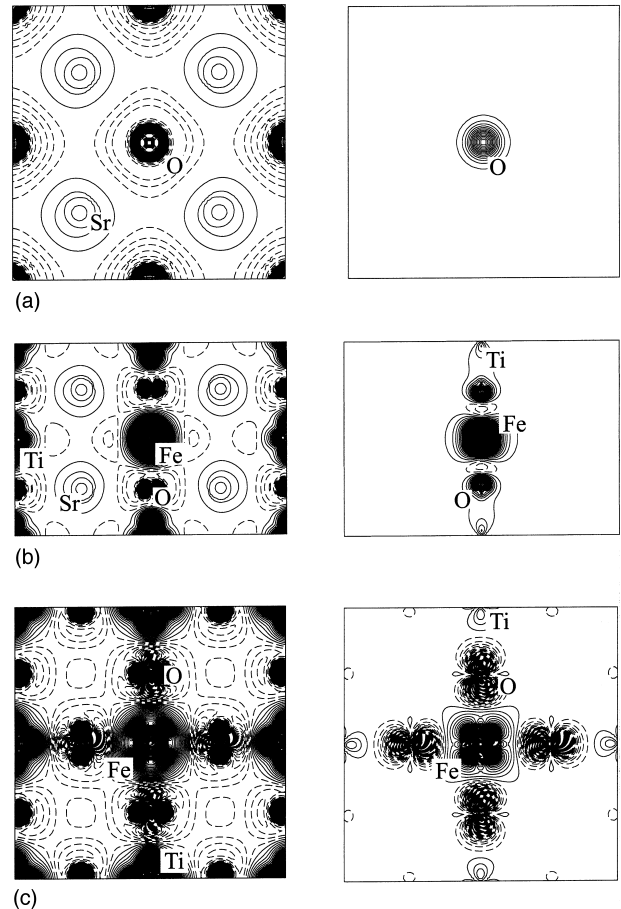


FIG. 2. (a) The electronic density plots for the (010) cross section of Fe and nearest ions in  $\text{SrTiO}_3$  as calculated by means of HF method for the cyclic cluster of 160 atoms. Isodensity curves are drawn from  $-0.8$  to  $0.8$  e a.u.<sup>-3</sup> with an increment of  $0.0022$  e a.u.<sup>-3</sup>, (b) the same as (a) for the (001) section, (c) the same for the (110) section. Left panels are HF difference electron densities, right panels spin densities.

and indeed, found in the latter case a small additional energy decrease, down to 1.42 eV for the following asymmetrical displacements: 0.028 Å along the  $x,y$  axis and  $-0.052$  Å along the  $z$  axis, i.e., outward displacements of two O atoms are twice larger than those for four equatorial O atoms. Note that our UHF calculation effectively incorporates the spin-dependent electron correlation effects during the self-consistency loops and thus gives nearly the same results as HF with *a posteriori* (non-self-consistent) corrections for electron correlations.

As follows from Eq. (13), the total valence of the iron impurity  $V_{\text{Fe}}=3.3e$  correlates much better with the  $\text{Fe}^{4+}$  model than with the calculated Mulliken effective charge of  $2.59e$ . These effective charges  $q$  of atoms collected in Table IV demonstrate considerable *covalency effects*, well known for  $\text{ABO}_3$  perovskites.<sup>3</sup> In particular, in pure  $\text{SrTiO}_3$  the effective charges are  $q(\text{Ti})=2.54e$ ,  $q(\text{Sr})=1.84e$ , and  $q(\text{O})=-1.46e$ . The Ti-O bond order in a pure crystal is  $0.375e$ . When the two O atoms are displaced outwards from the Fe impurity along the  $z$  axis and thus approach the nearest Ti atoms, the Ti-O bond order increases up to  $0.489e$ .

The combination of a large lattice relaxation energy and relatively small O displacements is not surprising in the light of a considerable covalent bonding between the unpaired iron electrons occupying Fe  $3d$  orbitals and  $2p$  orbitals of four equatorial oxygen ions: the Fe-O $_{x,y}$  bond orders (Table V) increase upon mutual approach of these atoms from  $0.164e$  to  $0.235e$ . Analysis of the total electron density and spin density distribution (Fig. 2) shows that in HF calculation four unpaired electrons are well localized on the Fe ion.

Lastly, a comparison of the band structures for the cyclic cluster containing Fe impurity with that for a pure crystal clearly demonstrates that Fe impurity induces additional energy levels below the valence band (in the region around  $-20$  eV) and above the valence band, at around  $-2$  eV. These bands have practically no dispersion over the BZ which demonstrates that the defect is almost isolated.

## VI. CONCLUSIONS

In this paper, we suggested a regular method to check on the convergence of periodic defect calculations to the limit of the single defect. Any method is not completely universal, and ours has also its limitations. In particular, it does not work when incorporation of the lattice relaxation qualitatively changes the electron localization (e.g., for free electron and hole polarons). On the other hand, it could be very efficient for many impurities in insulators characterized by high symmetry and when calculating forces is computationally

expensive. We have demonstrated that the size of the cyclic cluster large enough for a correct reproduction of the perfect crystal depends on the particular quantum mechanical method; for  $\text{SrTiO}_3$  this means 80 atom cyclic clusters for the HF but 320 atoms for the DFT-PWGGGA. In the HF-defect calculations for the single  $\text{Fe}^{4+}$  impurity the cyclic cluster should be not smaller than 160 atoms. This is in contrast with many previous supercell calculations where as small as  $L8$  supercells were used without convergence analysis.

It should be mentioned here that HF typically overestimates the optical gap whereas DFT underestimates it. This can affect the electronic density distribution (chemical bond covalency) and defect level positions within the gap (even determined with respect to the valence band top). In this respect, the so-called *hybrid* HF-DFT methods widely used in the molecular chemistry, e.g., B3LYP, seem to be promising tools.<sup>42,43</sup> Such the hybrid functionals being based on the LCAO basis set are incorporated into the recent version of the CRYSTAL code.<sup>11</sup>

The present calculations have demonstrated the strong covalent bonding between unpaired electrons of Fe impurity and four nearest O ions relaxed towards an impurity. Positions of Fe energy levels in a  $\text{SrTiO}_3$  gap are very sensitive to the lattice relaxation which was neglected in previous studies. The predicted positions of the Fe energy levels with respect to the valence band top could be checked by means of the UPS spectroscopy whereas the local lattice relaxation around iron and its spin state—by means of the EXAFS. This is the more important since the single  $\text{Fe}^{4+}$  ions so far are not detected by ESR (only  $\text{Fe}^{4+}\text{-V}_\text{O}$  complexes were studied)<sup>1</sup> and their optical absorption bands at 2.1 and 2.8 eV (Ref. 2) are tentative. Note that our predicted high-spin state of  $\text{Fe}^{4+}$  impurity contradicts to previous semi-empirical and simple calculations ( $X_\alpha\text{-FeO}_6$  cluster calculation<sup>6</sup> and tight-binding calculation).<sup>5</sup> On the other hand, high spin state is indirectly supported by its observation for host Fe ions in  $\text{SrFeO}_3$  perovskite.<sup>44</sup> Lastly, the proposed total valency of Fe ( $3.3e$ ) much better correlates with the  $\text{Fe}^{4+}$  model of impurity than the (standard) Mulliken effective charge of  $2.6e$ .

## ACKNOWLEDGMENTS

The authors are indebted to E. Heifets, R. Eglitis, A. Postnikov, R. Dovesi, and J. Maier for stimulating discussions. This study was partly supported by the European Center for Advanced Materials and Technology in Riga, Latvia (Contract No. ICA1-CT-2000-7007 to E.K.) and DFG (R.E. and G.B.).

\*E-mail address: ekotomin@fkf.mpg.de On leave from Institute for Solid State Physics, 8 Kengaraga str., Riga LV-1063, Latvia.

<sup>1</sup>O. F. Schirmer, W. Berlinger, and K. A. Müller, *Solid State Commun.* **16**, 1289 (1975); C. Ang, Z. Yu, Z. Jing, P. Lunkenheimer, and A. Loidl, *Phys. Rev. B* **61**, 3922 (2000).

<sup>2</sup>R. Waser, T. Bieger, and J. Maier, *Solid State Commun.* **76**, 1077 (1990).

<sup>3</sup>H.-J. Donnerberg, *Phys. Rev. B* **50**, 9053 (1994).

<sup>4</sup>A. V. Postnikov, A. I. Poteryaev, and G. Borstel, *Ferroelectrics* **206**, 69 (1998).

<sup>5</sup>M. O. Selme, P. Pecheur, and G. Toussaint, *J. Phys. C* **17**, 5185 (1984).

<sup>6</sup>F. M. Michel-Calendini and K. A. Müller, *Solid State Commun.* **40**, 255 (1981).

<sup>7</sup>P. Moretti and F. M. Michel-Calendini, *Phys. Rev. B* **34**, 8538 (1986).

- <sup>8</sup>H.-J. Donnerberg, *Atomic Simulations of Electro-Optical and Magneto-Optical Materials*, Vol. 151 of Springer Tracts in Modern Physics (Springer, Berlin, 1999).
- <sup>9</sup>P. Deak, *Phys. Status Solidi B* **217**, 9 (2000).
- <sup>10</sup>C. Sousa, Coen de Graaf, and F. Illas, *Phys. Rev. B* **62**, 10 013 (2000).
- <sup>11</sup>*Quantum-Mechanical Ab-initio Calculations of the Properties of Crystalline Materials*, Vol. 67 of Lecture Notes in Chemistry, edited by C. Pisani (Springer, Berlin, 1996), p. 327; V. R. Saunders, R. Dovesi, C. Roetti, M. Causá, N. M. Harrison, R. Orlando, and C. M. Zicovich-Wilson, *CRYSTAL 98 User's Manual*, Universita di Torino, Torino, 1998, <http://www.dl.ac.uk/TCS/Software/Crystal> and <http://www.ch.unito.it/ifm/teorica/crystal.html>
- <sup>12</sup>M. J. Pushka, S. Pöykkö, M. Resola, and R. M. Nieminen, *Phys. Rev. B* **53**, 1318 (1998).
- <sup>13</sup>G. Makov, R. Shach, and M. C. Payne, *Phys. Rev. B* **53**, 15 513 (1996).
- <sup>14</sup>P. Ordejon, *Phys. Status Solidi B* **217**, 335 (2000).
- <sup>15</sup>G. Mallia, R. Orlando, C. Roetti, P. Ugliengo, and R. Dovesi, *Phys. Rev. B* **63**, 235102 (2001).
- <sup>16</sup>A. Lichanot, P. Baranek, M. Merawa, R. Orlando, and R. Dovesi, *Phys. Rev. B* **62**, 12 812 (2000).
- <sup>17</sup>T. Bredow, R. A. Evarestov, and K. Jug, *Phys. Status Solidi B* **222**, 495 (2000).
- <sup>18</sup>C. Pisani, R. Dovesi, C. Roetti, M. Causa, R. Orlando, S. Casassa, and V. R. Saunders, *Int. J. Quantum Chem.* **77**, 1032 (2000).
- <sup>19</sup>C. Pisani, U. Birkenheuer, F. Cora, R. Nada, and S. Casassa, *EMBED-96 Users Manual*, University of Torino, 1996.
- <sup>20</sup>V. Sulimov, S. Casassa, C. Pisani, J. Garapon, and B. Poumellec, *Modell. Simul. Mater. Sci. Eng.* **8**, 763 (2000).
- <sup>21</sup>P. Baranek, G. Pinarello, C. Pisani, and R. Dovesi, *Phys. Chem. Chem. Phys.* **2**, 3893 (2000).
- <sup>22</sup>D. J. Chadi and M. L. Cohen, *Phys. Rev. B* **8**, 5747 (1973).
- <sup>23</sup>R. A. Evarestov and V. P. Smirnov, *Phys. Status Solidi B* **119**, 9 (1983).
- <sup>24</sup>J. Moreno and J. M. Soler, *Phys. Rev. B* **45**, 13 891 (1992).
- <sup>25</sup>R. A. Evarestov and V. P. Smirnov, *J. Phys. C* **9**, 3023 (1997).
- <sup>26</sup>R. A. Evarestov, V. A. Lovchikov, and I. I. Tupitsyn, *Phys. Status Solidi B* **117**, 417 (1983).
- <sup>27</sup>R. A. Evarestov and I. I. Tupitsyn, *Russ. J. Phys. Chem.* **74**, S363 (2000); *Phys. Solid State* **44**, 1656 (2002).
- <sup>28</sup>R. A. Evarestov and V. P. Smirnov, *Site Symmetry in Crystals: Theory and Applications*, 2nd ed., Vol. 108 of Springer Series in Solid State Sciences (Springer-Verlag, Berlin, 1997).
- <sup>29</sup>R. A. Evarestov and V. P. Smirnov, *Phys. Status Solidi B* **215**, 949 (1999).
- <sup>30</sup>T. Bredow, G. Geudtner, and K. Jug, *J. Comput. Chem.* **22**, 89 (2001).
- <sup>31</sup>H. J. Monkhorst and J. D. Pack, *Phys. Rev. B* **13**, 5188 (1976).
- <sup>32</sup>J. P. Perdew and Y. Wang, *Phys. Rev. B* **45**, 13 244 (1992).
- <sup>33</sup>M. Causá and A. Zupan, *Chem. Phys. Lett.* **220**, 145 (1994).
- <sup>34</sup>S. Dall'Olio, R. Dovesi, and R. Resta, *Phys. Rev. B* **56**, 10 105 (1997).
- <sup>35</sup>Ph. Baranek, C. M. Zicovich-Wilson, C. Roetti, R. Orlando, and R. Dovesi, *Phys. Rev. B* **64**, 125102 (2001).
- <sup>36</sup>P. Durand and P. Barthelat, *Theor. Chim. Acta* **38**, 283 (1975).
- <sup>37</sup>P. J. Hay and W. R. Wadt, *J. Chem. Phys.* **82**, 284 (1985).
- <sup>38</sup>R. A. Evarestov, A. V. Leko, and V. A. Veryazov, *Phys. Status Solidi B* **210**, R3 (1998); V. A. Veryazov, A. V. Leko, and R. A. Evarestov, *Phys. Solid State* **41**, 1286 (1999); R. A. Evarestov and V. A. Veryazov, *Theor. Chim. Acta* **81**, 95 (1991).
- <sup>39</sup>M. Catti, G. Valerio, and R. Dovesi, *Phys. Rev. B* **51**, 7441 (1995).
- <sup>40</sup>R. C. Bochicchio and H. F. Reale, *J. Phys. B* **26**, 4871 (1993).
- <sup>41</sup>*Ferroelectrics and Related Substances*, edited by K.-H. Hellwege and A. M. Hellwege, Landolt-Börnstein, New Series, Group 3, Vol. 3 (Springer-Verlag, Berlin, 1969).
- <sup>42</sup>J. Muscat, A. Wander, and N. M. Harrison, *Chem. Phys. Lett.* **342**, 397 (2001).
- <sup>43</sup>E. Heifets, R. Eglitis, E. A. Kotomin, J. Maier, and G. Borstel, *Surf. Sci.* **513**, 211 (2002).
- <sup>44</sup>M. Takano, T. Okita, N. Nakayama, Y. Bando, Y. Takeda, O. Yamamoto, and J. B. Goodenough, *J. Solid State Chem.* **73**, 140 (1988).